Developmental Biology 331 (2009) 199–209

Contents lists available at ScienceDirect

Developmental Biology

journal homepage: www.elsevier.com/developmentalbiology

Antagonistic interactions among Plexins regulate the timing of intersegmental vessel formation

Ryan E. Lamont, Erica J Lamont, Sarah J Childs *

Department of Biochemistry and Molecular Biology, University of Calgary, Calgary AB, Canada T2N 4N1

ARTICLE INFO

Article history:
Received for publication 15 September 2008
Revised 28 April 2009
Accepted 29 April 2009
Available online 5 May 2009

Keywords:
Zebrafish
Semaphorin3e
PlexinB2
PlexinD1
Endothelial cell
Vessel
Patterning
Angioblast

ABSTRACT

The angioblast is an embryonic endothelial cell precursor that migrates long distances to reach its final position, navigating by sensing attractive and repulsive cues from the environment. Members of the semaphorin family have been implicated in controlling the behaviour of angioblast tip cells through repulsive signalling in vitro, but their in vivo roles are less clear. Here we show that zebrafish *semaphorin3e* (*sema3e*) is expressed by endothelial cells of the dorsal aorta, primary motoneurons, and endodermal cells. Further, loss of Sema3e leads to delayed exit of angioblasts from the dorsal aorta in ISV formation. Through transplant analysis, we show that Sema3e acts autonomously and non-autonomously in angioblasts to modulate interactions among themselves. The semaphorin receptors, PlexinD1 and PlexinB2, are expressed by zebrafish angioblasts. Loss of *plxnB2* results in delayed ISV sprouting identical to that seen in *sema3e* morphants, while loss of *plexinD1* in *out of bounds* (*obd*) mutants results in precocious ISV sprouting. Loss of either *sema3e* or *plxnB2* in *obd* mutants generates an intermediate phenotype, suggesting that PlxnD1 and Sema3e/PlxnB2 antagonize each other to control timing of ISV sprouting. Consistent with this observation, we show that PlxnB2 acts cell autonomously in endothelial cells. This suggests a model where multiple semaphorin–plexin interactions control angioblast sprouting behaviour.

Introduction

We are interested in determining the signals that pattern the development of the vasculature. Zebrafish intersegmental vessels (ISVs) are an excellent system to study how alterations in signals result in subtle changes in cell morphology and behaviour because they are only one cell in diameter and three or four cells in length (Childs et al., 2002; Siekmann and Lawson, 2007). Furthermore, transgenic zebrafish expressing GFP in angioblasts can be used to trace vascular development in vivo in the transparent embryo (Choi et al., 2007; Cross et al., 2003; Lawson and Weinstein, 2002).

During zebrafish development, angioblasts are specified in the bilateral lateral posterior mesoderm, after which they migrate to the midline where they undergo tubulogenesis to form the dorsal aorta and posterior cardinal vein by the 17 somite stage (17S) (Eriksson and Lofberg, 2000). Angioblasts then sprout from the dorsal aorta to form the ISVs at 20S in an anterior to posterior wave, following the developmental maturation of somites. The ISVs grow dorsally from the dorsal aorta, restricted medially and dorsally by the notochord and laterally, rostrally, and caudally by the somites. When the ISVs reach the dorsal region of the embryo, the cells take on a "T"-shaped morphology and fuse to adjacent cells to form the dorsal longitudinal anastomotic vessel (DLAV) (Childs et al., 2002).

Migrating angioblasts assume one of two cellular identities: a tip cell or a stalk cell (Gerhardt et al., 2003; Siekmann and Lawson, 2007). The tip cell is analogous to the axon growth cone as it senses the extracellular environment for attractive and repulsive growth cues through filopodial projections. The stalk cell is non-migratory, non-proliferative, undergoes lumenization, and has a decreased number of filopodia. The stalk cell develops from the tip cell after it reaches its final position. In the zebrafish, once ISV tip cells reach the dorsal aspect of the embryo, cells from adjacent ISVs come into contact with each other and reciprocal signalling through the Notch signalling pathway suppresses filopodial extension and transforms tip cells to a stalk cell identity (Hellstrom et al., 2007; Leslie et al., 2007; Siekmann and Lawson, 2007).

Some of the signals guiding the migration of ISV angioblasts have been determined. We previously reported the *out of bounds* (*obd*) zebrafish genetic mutant with a guidance defect resulting in precocious and spatially unrestricted migration of angioblasts from the dorsal aorta as early as 17S, together with the formation of ectopic connections among vessels (Childs et al., 2002). We identified the genetic lesion in *obd* mutants by positional cloning and found a mutation in the vascular-specific *plexinD1* (*plxnD1*) receptor (Torres-Vazquez et al., 2004). Mouse embryos deficient for PlxnD1 have a similar phenotype and also exhibit excessive ISV branching (Gitler et al., 2004; Gu et al., 2005). Plexins serve as receptors for semaphorin

Abbreviations: ISV, intersegmental vessel; S, somite stage; hpf, hours post fertilization; Semaphorin, sema; Plexin, plxn; wild type, wt.

* Corresponding author. Fax: +1 403 270 2211.
E-mail address: schilds@ucalgary.ca (S.J. Childs).

0012-1606/$ – see front matter © 2009 Elsevier Inc. All rights reserved.
doi:10.1016/j.ydbio.2009.04.037

(sema) ligands. There are currently nine different plexin receptors and five classes of semaphorin ligands known in vertebrates (Eichmann et al., 2005; Takahashi et al., 1999; Tamagnone et al., 1999; Winberg et al., 1998). Of these, PlxnA2, PlxnB1, PlxnB2, PlxnB3, PlxnD1, Sema3a and Sema3c are expressed in endothelial cells (Banu et al., 2006; Basile et al., 2004; Herzog et al., 2005; Serini et al., 2003; Toyofuku et al., 2007).

Semaphorin–PlxnD1 signalling is thought to contribute to the fine behaviour of angioblast tip cells as they migrate by the transduction of repulsive signals. Semaphorin 3E (Sema3E) is a secreted semaphorin that is activated by furin proteolytic cleavage and dimerization (Adams et al., 1997; Christensen et al., 2005). To date, most work on Sema3E has concentrated on its role in nervous system development where it repulses retinal axons (Steffensky et al., 2006; Steinbach et al., 2002), hippocampal axons (Pozas et al., 2001), and sensory axons (Miyazaki et al., 1999a, b). Interestingly, Sema3E exerts different responses in different PlxnD1-expressing neuronal populations depending on the presence or absence of the Neuropilin-1 (Nrp1) co-receptor. In corticofugal and striatonigral neurons, Sema3E/PlxnD1 signalling acts repulsively in the absence of Nrp1, and acts attractively on subiculo-mamillary neurons that express Nrp1 (Chauvet et al., 2007). Sema3e also plays a similar role in vascular development. Expression of Sema3e in PlxnD1-expressing cultured endothelial cells collapses filopodia, while misexpression in the chick somite repulses the growth of endogenous vessels (Gu et al., 2005). PlexinD1 binding to Sema3E is neuropilin-independent since Sema3E binds mouse ISV cells in the absence of Nrp, and deletion of the semaphorin binding domain of Nrp1 does not affect ISV patterning (Gu et al., 2005). Thus, it has been proposed that Sema3E is the primary repulsive ligand for PlxnD1 in ISV patterning independent of Nrp1 (Gu et al., 2005). Interestingly, other studies have shown that cleaved and dimerized Sema3E promotes the migration of endothelial cells in vitro (Christensen et al., 2005), suggesting that Sema3E can also act as an attractant to endothelial cells in a context dependent manner.

PlxnB2 is also expressed in endothelial cells (Toyofuku et al., 2007), however, its role in vascular development has not been explored. B-type plexins differ from other members of the plexin family due to the presence of a PDZ-binding motif in their cytoplasmic C-terminus that mediates the physical interaction with two guanine nucleotide exchange factors (GEFs): PDZ-RhoGEF and Leukemia-associated Rho GEF (LARG) (Aurandt et al., 2002; Perrot et al., 2002; Swiercz et al., 2002). Like semaphorins, PlxnB2 undergoes extracellular proteolytic cleavage to increase ligand binding affinity (Artigiani et al., 2003). Previous studies have shown that PlxnB2 controls the migration, patterning, differentiation and proliferation of granule cells in the cerebellum through its high affinity ligand Sema4c (Deng et al., 2007; Friedel et al., 2007). It also promotes the outgrowth of neurites in primary cerebellar neurons in mice and mediates cell aggregation (Hartwig et al., 2005).

Our previous work with PlxnD1 suggested that it, along with its Sema3a2 ligand, is involved in the timing of angioblast exit from the dorsal aorta to form the ISVs (Torres-Vazquez et al., 2004). Here we show that Sema3e plays a novel autocrine role in the promotion of ISV sprouting in zebrafish. Further, we have identified PlxnB2 as a plexin that genetically interacts with Sema3e in the promotion of angioblast exit. We also show genetic evidence that Sema3e/PlxnB2 and PlxnD1 modulate the timing of angioblast exit through two independent pathways.

Materials and methods

Embryo generation and staging

Zebrafish embryos were raised at 28.5 °C according to Westerfield (1995) in E3 embryo buffer and staged according to Kimmel et al. (1995). To block pigment formation, 0.003% phenylthiocarbamide (PTU; Sigma, St. Louis, MO) was added to the embryo buffer at 4 hours post fertilization (hpf). Transgenic and mutant zebrafish lines have been previously described: *Tg(kdr:GFP)*^{la116} (Choi et al., 2007), *Tg (fli1a:EGFP)*^{y1} (Lawson and Weinstein, 2002), *obd*^{fov1b}, and *obd*^{fv109} (Childs et al., 2002).

sema3e and plxnB2 cloning and in situ hybridization

Full length coding sequence for *sema3e* was obtained by identifying the translational start site in the partial 5′ *sema3e* clone AW280261. To obtain 3′ sequence, *sema3e* was amplified from a 50 hpf RACE library (Clontech, Mountain View, CA) using the Advantage 2 PCR system (Clontech) and the primers 5′-GGA GCT GAA CAG GAC GTG GGT GTT CCA GG-3′ and 5′-CCA TCC TAA TAC GAC TCA CTA TAG GGC-3′ followed by nested amplification with 5′-GGA GAG GGC CGT CTG CAG CAA TAC ACC ATG-3′ and 5′-ACT CAC TAT AGG GCT CGA GCG GC-3′. This resulted in a 2.7 kb fragment containing 2.1 kb coding sequence and 0.6 kb of 3′ untranslated region, which has been deposited in GenBank under accession EF656360. Template for in vitro transcription was obtained by digestion of this clone with XbaI (Invitrogen, Carlsbad, CA) and transcription with SP6 RNA polymerase (Promega, Madison, WI).

We identified zebrafish *plxnB2* from the EST clones CT675855, DN857106, EB955063, and CD597409. The primers 5′-ATG CAT TCA TCA GCC AGA GC-3′ and 5′-TGG CAG TCA TGG CTTT GGC A-3′ were used to generate a 872 bp fragment which was subcloned into pCRII (Invitrogen) and used as a template for an in situ probe. In situ hybridization was performed as above. Complete plxnB2 coding sequence was identified using predicted sequence from ENSEMBL, and amplified from cDNA using the primers 5′-ATG GCG TGG AGG GCC CTG-3′ and 5′-C TAA AGG TCG GTG ACT TTA TTC TCC-3′ generating a 5.6 kb fragment which has been deposited in GenBank under accession number EU743740.

Whole-mount in situ hybridization was performed as described in Jowett and Lettice (1994). For photography, embryos were embedded in 3% methylcellulose and photographed using a Zeiss Axiocam HRc. For sectioning, embryos were embedded in JB4 medium (Polysciences, Warrington, PA) and sectioned at 7 μM using a Leica microtome.

Morpholino and DNA injections

Morpholinos (MO) against the *sema3e* start codon (*sema3e*^{ATG}; ATG underlined) 5′-TGAAAGTCCACACACCCCACGCCAT-3′ or exon 3/intron 3 splice boundary (*sema3e*^{e3i3}) 5′-AATATCAGCTTTACCTTC-TCTCTGC-3′ were obtained from Gene Tools LLC (Corvallis, OR). Efficacy of *sema3e*^{e3i3} splice morpholino was determined by RT-PCR using the forward primer 5′-TCCTGTACTCCCTCAATCTG-3′ and reverse primer 5′-CATGCCAGCAGATGAGTGCT-3′, resulting in complete mis-splicing at a dose of 1.9 ng per embryo (Supplemental Fig. 1). The *sema3e*^{ATG} morpholino was used at a dose of 3.9 ng. Morpholinos were diluted in 0.3× Danieau solution and injected into 1–8 cell zebrafish embryos. To assess non-specific cell death, morpholino-injected embryos were placed in 5 μg/mL acridine orange (Sigma) in E3 embryo buffer for 30 min. There was no off-target cell death apparent with the *sema3e*^{ATG} morpholino at this dose (Supplemental Fig. 2).

Full length coding sequence for *sema3e* was amplified by PCR with primers 5′-AAA AAG CAG GCT TCA CCA TGG CGT GGG GTG TGT GGA C-3′ and 5′-AGA AAG CTG GGT GCT ACT GTC CCG GTG TGT GT-3′ incorporating the attB1 and attB2 adapter sequences for Gateway cloning (Invitrogen). Multisite Gateway cloning using the Tol2 kit (Kwan et al., 2007) was used to clone *lmo2:sema3e:IRES-mEGFP, kdr: sema3e:IRES-mEGFP* into *pDestTol2pA2* (Kwan et al., 2007). The *kdr* and 2.5 kb *lmo2* promoters have been described (Choi et al., 2007; Cross et al., 2003; Du et al., 2003; Zhu et al., 2005). For expression, 23.8 pg of circular DNA and 47.5 pg of Tol2 transposase mRNA were injected just beneath the cell of 1–2 cell zebrafish embryos.

Morpholinos against *plxnB2* were targeted against the intron 10/exon 11 splice boundary (*plxnB2*^{i10e11}) 5′-GGC TCT TTG TCA TAC GCA AAC TGG C-3′ or the exon 4/intron 4 splice boundary (*plxnB2*^{e4i4}) 5′-ATC ATT CTT AAC AGA CTT ACC GGC C-3′. Efficacy of *plxnB2*^{i10e11} was determined by RT-PCR using the primers 5′-GGC CGA TGG GTT AAA GTA CA-3′ and 5′-TTT CTC CTT CCA CCA ACA CC-3′, resulting in complete mis-splicing at a dose of 16 ng per embryo (Supplemental Fig. 1). *plxnB2*^{e4i4} was injected at a dose of 12 ng per embryo and gave an identical phenotype. Acridine orange staining revealed mild off-target neural cell death in *plxnB2*^{i10e11} morphants (Supplemental

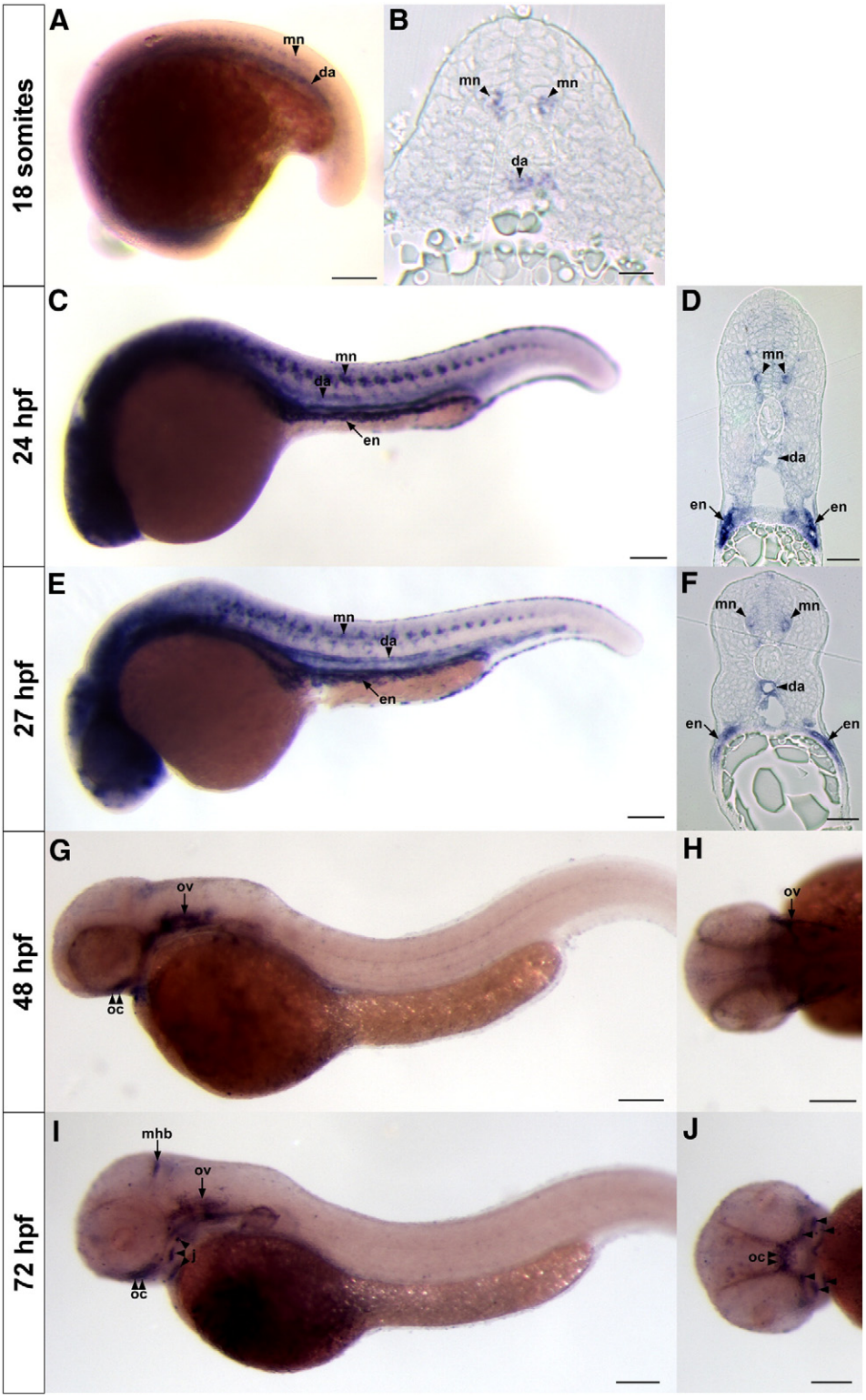

Fig. 1. Dynamic expression of zebrafish *sema3e*. (A, B). At 18 somites, *sema3e* is expressed in one primary motoneuron per somite (mn) and the dorsal aorta (da). (C–F) At 24 and 27 hpf, continued expression is observed in a single primary motoneuron and the dorsal aorta, with expression now observed in endodermal tissue ventral to the pronephric ducts (en). (G, H) By 48 hpf, only neural expression of *sema3e* is observed. Signal is seen in the otic vesicle (ov) and optic chiasm (oc); persisting through 72 hpf (I, J) where expression is also observed at the midbrain–hindbrain boundary (mhb) and in developing jaw structures (j). (A, C, E, G–J) are wholemount images while (B, D, F) are transverse sections. (A, C, E, G, I) are lateral views, (H) is dorsal view, (J) is ventral view. Scale bar in A is 325 μm, B is 10 μm, C, E, G–J is 400 μm, and D, F is 30 μm.

Fig. 2), however co-injection of morpholino against p53 (5′-GCG CCA TTG CTT TGC AAG AAT TG-3′) (Robu et al., 2007) did not alter the vascular phenotype of *plxnB2*^{i10e11} morphants (data not shown), indicating that the vascular phenotype is specific to PlxnB2 knock-down, and not to off-target cell death. *sema3e*/*plxnB2* double morphants were obtained using *sema3e*^{ATG} and *plxnB2*^{i10e11} at 1.9 ng and 4 ng, respectively.

Counting of ISV sprouts

ISV sprouts were counted in morpholino-injected, uninjected, and *obd* crosses on a *Tg(kdr:GFP)*^{la116} background at 24 hpf after light fixation in 4% PFA for 45 min. The total numbers of ISV sprouts on one side of an embryo were counted under epi-fluorescence.

Cell transplantation

For cell transplantation, *Tg(kdr:GFP)*^{la116} donor embryos were injected with 10,000 MW rhodamine-dextran (Invitrogen) with or without 3.9 ng of *sema3e*^{ATG} or 16 ng of *plxnB2*^{i10e11} morpholino and allowed to grow in 0.3× Danieau solution. Some recipient embryos were also injected with 3.9 ng of *sema3e*^{ATG} or 16 ng of *plxnB2*^{i10e11} morpholino. At 30–50% epiboly, 50–100 cells were transplanted from donor embryos into the dorsal margin of non-GFP recipient embryos in the presence of 1× Danieau solution. Donor and recipient embryos were then allowed to develop in 0.3× Danieau solution and 2.5× Penicillin/Streptomycin. At 24 hpf, recipient embryos were sorted for the presence of *kdr-GFP* positive endothelial cells, mounted in 0.5% low melt agarose (Invitrogen) and photographed using a Zeiss SV11 epifluorescent microscope (Carl Zeiss Inc., Thornwood, NY). Total numbers of ISV and dorsal aorta cells were counted in wt>wt ($n=342$ cells from 26 embryos), wt>3e MO ($n=583$ cells from 43 embryos), 3e MO>wt ($n=326$ cells from 40 embryos), wt>plxnB2 MO ($n=234$ cells from 17 embryos), and plxnB2 MO>wt ($n=179$ cells from 20 embryos). Any errors in counting would be expected to affect all experimental groups equally. The proportion of cells contributing to the PCV did not differ between the various transplantation experiments and were not included in our analyses. Each experiment was performed at least twice to ensure reproducibility. Transplanted embryos containing high numbers of cells of endodermal or ectodermal origin were not included in analyses as these are potential non-autonomous sources of Sema3e.

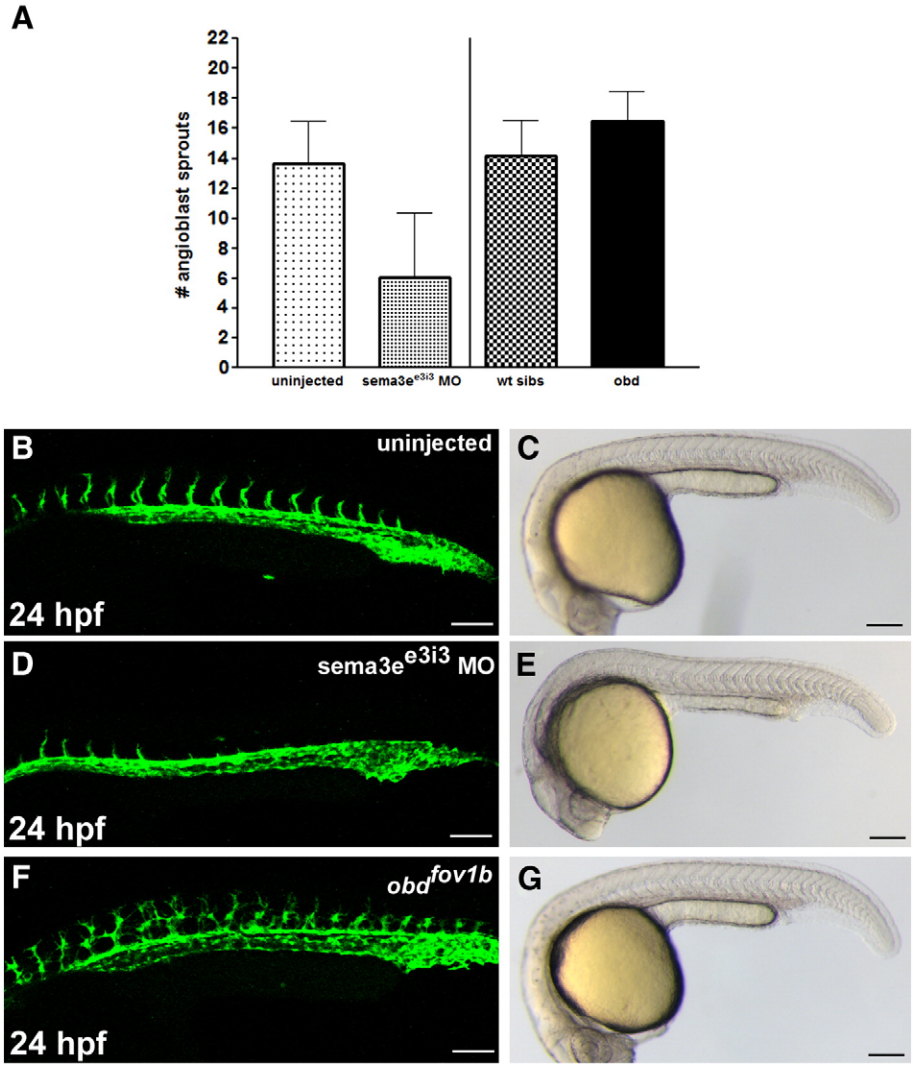

Fig. 2. Intersegmental sprouting is delayed in *sema3e*^{e3i3} morphants and is precocious in *obd* mutants. (A) Graphical representation of the mean number and standard deviation of angioblast sprouts observed in *sema3e*^{e3i3} morphants and *obd*^{fov1b} mutants as compared to control embryos. Confocal (B, D, F) and corresponding white light images (C, E, G) of uninjected (B, C), *sema3e*^{e3i3} morphants (D, E), and *obd*^{fov1b} mutants (F, G) at 24 hpf on a *Tg(kdr:GFP)*^{la116} genetic background. Scale bar in B, D, F is 100 μm and C, E, G is 500 μm.

Results

sema3e is dynamically expressed in diverse tissues

We identified the zebrafish *sema3e* ortholog using the UCSC Zebrafish Genome Browser (http://genome.ucsc.edu). We identified only a single *sema3e* gene in zebrafish, unlike many genes which are present in two copies in the zebrafish genome. Expression analysis by wholemount in situ hybridization showed that *sema3e* was expressed in one primary motoneuron per somite, as well as the dorsal aorta at 18S (Figs. 1A, B). At 24 hpf, expression persisted in a single primary motoneuron per somite, as well as in the endoderm beneath the pronephric duct at both 24 and 27 hpf (Figs. 1C–F). Vascular, endodermal, and motoneuron expression was not observed at 48 hpf. At this time, expression was seen in the otic vesicle and the optic chiasm (Figs. 1G, H) as previously reported (Callander et al., 2007). Expression of *sema3e* was maintained in the optic chiasm and other neural structures at 72 hpf, when expression in developing jaw structures appeared (Figs. 1I, J).

Loss of Sema3e results in delayed ISV sprouting

To determine the role of Sema3e in the development of the embryonic vasculature, we injected morpholino antisense oligonucleotides targeted against the translational start site (*sema3e*^{ATG}) or the splice junction between exon 3 and intron 3 (*sema3e*^{e3i3}) into transgenic *Tg(kdr:GFP)*^{la116} zebrafish embryos expressing GFP in all endothelial cells. Both morpholinos resulted in an identical phenotype and were used interchangeably. Complete mis-splicing of *sema3e* was seen at a dose of 1.9 ng of *sema3e*^{e3i3} (Supplemental Fig. 1). Further, cell death due to non-specific morpholino effects was assayed using acridine orange and no increase of cell death compared to uninjected controls was observed (Supplemental Fig. 2).

Previously, we reported that *obd* embryos show precocious angioblast sprouting at 17S, when compared to wild type angioblasts which begin sprouting at 20S (Childs et al., 2002). As Sema3E has been proposed to be the primary ligand for PlxnD1, we expected that down regulation of zebrafish *sema3e* would also result in precocious angioblast sprouting. Thus, we counted angioblast sprouts in *sema3e* morphants, *obd* mutants, and uninjected controls or wild type siblings, respectively, at 24 hpf. The sprouts on one side of the embryo were counted in uninjected embryos or *sema3e*^{e3i3} morphants on a *Tg(fli1:nEGFP)*^{17} background, and wild type sibling or *obd*^{fov1b} mutants on a *Tg(kdr:GFP)*^{la116} background. At 24 hpf, uninjected embryos had an average of 13.6 ± 2.8 sprouts (n = 28) (Figs. 2A, B). *sema3e*^{e3i3} morphants showed a significant delay in sprouting in that they had an average of 6.1 ± 4.3 sprouts per embryo (n = 59) (Figs. 2A, D). This delay showed high penetrance as 78% of *sema3e*^{e3i3} morphants had fewer than 10 angioblast sprouts per embryo, while only 7% of control embryos had fewer than 10 per embryo at this time. This delay is not permanent suppression of sprouting as *sema3e* morphants had an equivalent number of ISVs past the horizontal myoseptum as uninjected controls by 30 hpf (data not shown). This delay in sprouting was also not due to general developmental delay as the number of somites that had formed (a measure of developmental stage) is equal in both groups (Figs. 2C, E).

As expected, the average number of angioblast sprouts per embryo in *obd*^{fov1b} mutants was greater than that of their wild type siblings at 24 hpf (16.5 ± 1.9 (n = 94) versus 14.2 ± 2.3 (n = 90) sprouts per embryo, respectively) (Figs. 2A, F, G). Thus, loss of Sema3e results in delayed angioblast sprouting, while loss of PlxnD1 results in precocious sprouting. These are unexpectedly opposite phenotypes suggesting that they do not function as ligand and receptor pair in this aspect of vascular morphogenesis.

PlxnB2 genetically interacts with Sema3e

As we showed above, loss of PlxnD1 or Sema3e signalling results in opposite timing of angioblast sprouting phenotypes, suggesting an additional plexin expressed in angioblasts can act as a receptor for Sema3e. Thus, we identified all plexin molecules from the zebrafish genome and performed an in situ hybridization screen at 24 hpf to identify plexins expressed by endothelial cells (data not shown). Although PlxnB1, PlxnB2, and PlxnB3 have all been reported previously to be expressed by cultured endothelial cells (Toyofuku et al., 2007), we did not find expression of either *plxnB1* or *plxnB3* in endothelial cells (data not shown). However, we did find that *plxnB2* is expressed ubiquitously, with increased expression in the region of the ventral trunk (Figs. 3A, B). Thus, we chose to further examine the potential role of PlxnB2.

To determine the function of PlxnB2 in vascular development, we injected *Tg(kdr:GFP)*^{la116} embryos with two morpholinos against *plxnB2* (*plxnB2*^{i10e11} and *plxnB2*^{e4i4}) and achieved complete mis-splicing at doses of 16 ng and 12 ng, respectively (Supplemental Fig. 1). Non-specific cell death was determined using acridine orange and was determined not to affect the morphant vascular phenotype as co-injection of the *plxnB2*^{i10e11} and p53 morpholinos gave an identical vascular phenotype as *plxnB2*^{i10e11} morpholino alone (Supplemental Fig. 2 and data not shown). Both morpholinos gave an identical phenotype of delayed angioblast sprouting as compared to wild type (Figs. 3E, F, and data not shown), similar to that seen in *sema3e* morphants. At 24 hpf, uninjected embryos have an average of 16.0 (±3.5) sprouts per embryo (n = 110) while *plxnB2*^{i10e11}morphants had an average of only 3.7 (±2.9) sprouts per embryo (n = 110) (Figs. 3E, F, I). This phenotype was highly penetrant as 98.1% of *plxnB2*^{i10e11} morphants had fewer than 10 angioblast sprouts per embryo compared to only 5.5% in uninjected controls. Delayed ISV angioblast sprouting in *plxnB2*^{i10e11} morphants was not caused by general embryonic delay as the number of somites in uninjected controls and *plxnB2*^{i10e11} morphants were equal (Figs. 3C, D). Further, the delay of ISV growth in *plxnB2* morphants was determined by counting the number of ISVs sprouted past the horizontal myoseptum in 30 hpf control embryos and then determining the amount of time required for morphants to reach the equivalent stage. Using this method, we determined that ISV growth in *plxnB2* morphants is delayed 6 h compared to uninjected controls (data not shown).

The phenotypic similarity between *plxnB2* and *sema3e* (Figs. 3F, G) morphants suggests that these two molecules could be a receptor–ligand pair. To test this, we co-injected both *sema3e*^{ATG} and *plxnB2*^{i10e11} morpholinos together to observe if full knockdown of both genes simultaneously resulted in an exacerbated sprouting phenotype. However, co-injection of these two morpholinos resulted in complete embryo death, even with the addition of morpholino against p53 to block off-target cell death (data not shown). Therefore, suboptimal doses of *sema3e*^{ATG} and *plxnB2*^{i10e11} morpholinos (2 ng and 4 ng, respectively) were co-injected to determine partial loss of each gene could phenocopy the loss of each gene individually. Co-injection of suboptimal doses of morpholino resulted in delayed angioblast sprouting with an average of 5.2 (±5.2) sprouts per embryo (n = 70), while uninjected controls had an average of 15.3 (±2.0) sprouts per embryo (n = 71) (Figs. 3H, I). Each morpholino alone showed no phenotype at these doses (data not shown). These data provide strong evidence for a genetic interaction between Sema3e and PlxnB2.

PlxnD1 and PlxnB2/Sema3e act antagonistically to control timing of angioblast sprouts

Loss of PlxnD1 or Sema3e has opposite effects on timing of angioblast sprouting. To investigate if Sema3e and PlxnD1 antagonize each other we downregulated PlxnB2 and Sema3e in *obd* mutant

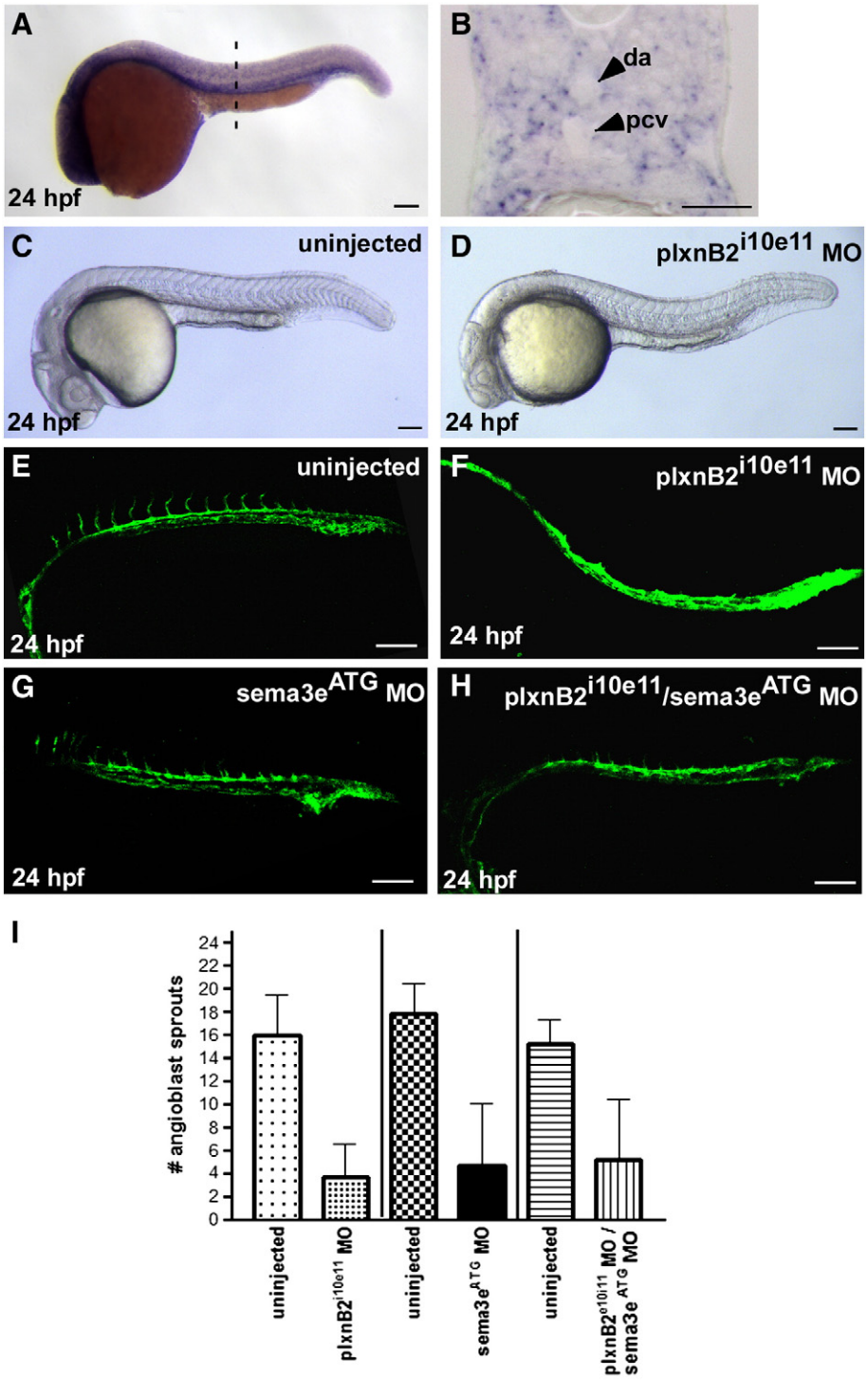

Fig. 3. Angioblast sprouting is delayed in *plxnB2*^{i10e11} and *plxnB2*^{i10e11}/*sema3e*^{ATG} morphants. (A–B) PlxnB2 expression analysis by in situ hybridization shows semi-ubiquitous expression with ventral enrichment in the region surrounding the axial vessels in wholemount (A) and cross section views (B). The dashed line in A indicates the level of the section in B. (C–D) White light images of control (C) and *plxnB2*^{i10e11} morphant (D) at 24 hpf. (E–H) Confocal images of uninjected (E), *plxnB2*^{i10e11} morphant (F), *sema3e*^{ATG} morphant (G), and *plxnB2*^{i10e11}/*sema3e*^{ATG} morphant (H) at 24 hpf on a *Tg(kdr:GFP)*^{la116} genetic background. (I) Graphical representation of the mean number and standard deviation of angioblast sprouts observed in *plxnB2*^{i10e11} morphants, *sema3e*^{ATG} morphants, and *plxnB2*^{i10e11}/*sema3e*^{ATG} morphants as compared to control embryos. Scale bar in A, C–H is 100 μm and 30 μm in B.

embryos and observed the timing of angioblast sprouts. *Obd*$^{fov01\text{-}b}$, $^{fs31\text{-}l}$ and ^{fv109k} alleles are functional nulls for PlexinD1 and are indistinguishable (Torres-Vazquez et al., 2004), and thus if PlxnB2 and PlxnD1 act in the same pathway, there should be no change in the *obd* phenotype when PlxnB2 expression is lost in the same animal.

Down-regulation of *plxnB2* in *obd* mutant embryos resulted in an additive phenotype with fewer angioblast sprouts (7.0 ± 5.7; $n = 44$) than in uninjected *obd* mutants (21.8 ± 2.0; $n = 43$) (Figs. 4A, C, E). Similarly, loss of Sema3e in *obd* mutant embryos resulted in fewer sprouts (10.6 ± 2.5; $n = 58$) than uninjected *obd* mutants (20.2 ± 1.8; $n = 62$). Notably, loss of Sema3e in *obd* mutants resulted in more angioblast sprouts than loss of Sema3e in their wild type sibs (10.6 ± 2.5 versus 3.9 ± 1.7 sprouts, respectively; Figs. 4B, D, F). Similar to our previous results, injection of *sema3e*^{ATG} morpholino into *obd* wild type sibs also resulted in delayed angioblast sprouting (3.9 ± 1.7; $n = 37$) compared to uninjected wild type sibs (16.6 ± 1.1; $n = 44$) at

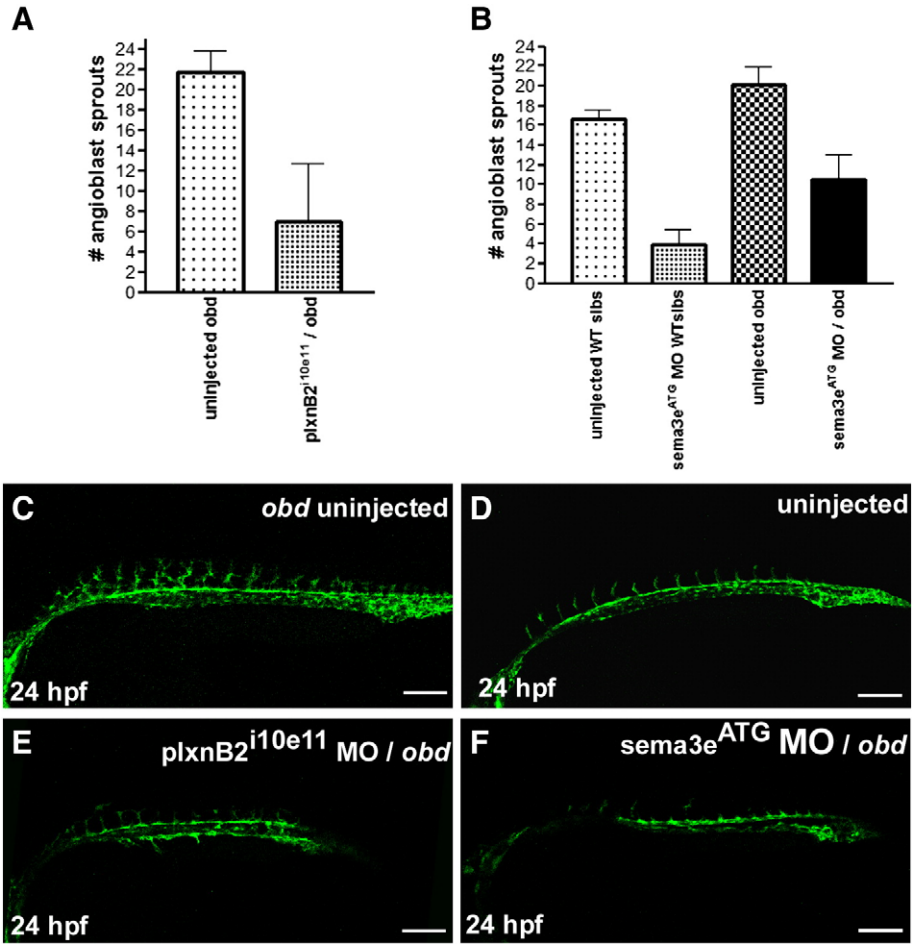

Fig. 4. Loss of plxnD1 and *sema3e*/*plxnB2* results in an intermediate angioblast sprouting phenotype (A) Graphical representation of the mean number and standard deviation of angioblast sprouts observed in *plxnB2*^{i10e11}/*obd* morphants as compared to control *obd* mutant embryos. (B) Graphical representation of the proportion of embryos exhibiting a given number of ISVs sprouts in uninjected *obd* wt sibs, *sema3e*^{ATG} MO/*obd* wt sib morphants, uninjected *obd* mutant embryos, and *sema3e*^{ATG} MO/*obd* morphants. (C–F) Confocal images of uninjected *obd* mutant (C), uninjected wt sibs (D), *plxnB2*^{i10e11}/*obd* morphants (E), and *sema3e*^{ATG}/*obd* morphants (F) at 24 hpf on a *Tg(kdr:GFP)*^{la116} genetic background. Scale bars in (C–F) are 100 μm.

24 hpf. The intermediate, additive phenotype when PlxinD1 and PlxinB2/Sema3e are lost in the same animal suggests that signalling from each receptor is distinct and that signalling downstream of each receptor likely antagonizes signalling from the other receptor.

Sema3e and PlxnB2 act autonomously in angioblasts

To further investigate the role of Sema3e and PlxnB2 in angioblast interactions, we sought to over-express Sema3e using the angioblast *lmo2* promoter (Zhu et al., 2005). However, injection of *sema3e* RNA or *lmo2:sema3e-IRES-GFP* DNA resulted in complete, early embryonic lethality (data not shown) which precluded us from determining the role of increased levels of Sema3e on angioblast behaviour. Injection of the control plasmid *lmo2:GFP-IRES-GFP* under the same conditions did not affect embryo survival (data not shown), suggesting that Sema3e itself is toxic at high levels. Consistent with this, relatively little morpholino is required for complete knockdown of *sema3e*. Since it was not technically feasible to over-express Sema3e in angioblasts, and there is no method for endothelial-specific deletion of genes in zebrafish, we undertook transplant analysis to determine the cell autonomy of Sema3e.

Previous data suggests that class 3 semaphorins can act cell autonomously on endothelial cells in culture (Serini et al., 2003). We hypothesized that if Sema3e was acting cell autonomously, transplantation of *sema3e* morphant angioblasts into wild type recipients would show delayed ISV sprouting, identical to that of *sema3e* morphants. As such, we predicted that few *sema3e* morphant cells would contribute to the ISVs and instead would remain in the region of the dorsal aorta. Conversely, we hypothesized that wild type angioblasts transplanted into a *sema3e* morphant recipient would act identical to wild type angioblasts transplanted into a wild type recipient.

When wild type *Tg(kdr:GFP)*^{la116} angioblasts were transplanted into wild type recipients, 59.1% of cells contributed to the dorsal aorta, while the remaining 40.9% contributes to the ISVs ($n = 342$ cells from 26 embryos; Figs. 5A, C)). Transplanted donor cells were also labelled with rhodamine-dextran to track the destination of donor cells and sort for embryos with few transplanted cells of endodermal or ectodermal origin, to remove possible sources of non-autonomous *sema3e* (Supplemental Fig. 3). As expected, transplantation of *sema3e*^{ATG} morphant *Tg(kdr:GFP)*^{la116} angioblasts into wild type recipients resulted in a substantial increase in the number of cells contributing to the dorsal aorta (79.8%) and a corresponding decrease in the number ISV cells (20.2%) ($n = 326$ from 40 embryos; $p<0.001$ by Chi-square test; Figs. 5A, E). These results suggest that *sema3e* acts cell autonomously in angioblasts.

Surprisingly, however, when we transplant wild type *Tg(kdr:GFP)*^{la116} angioblasts into *sema3e*^{ATG} morphant recipients, we also found an increase in cell numbers in the dorsal aorta (74.3% of transplanted angioblasts), while only 25.7% were ISV cells ($n = 583$ cells from 43 embryos; $p<0.002$ by Chi-square test; Figs. 5A, D), suggesting that Sema3e also acts in a non-cell autonomous manner on angioblasts. Given that *sema3e* is a secreted molecule, it is likely that one cell

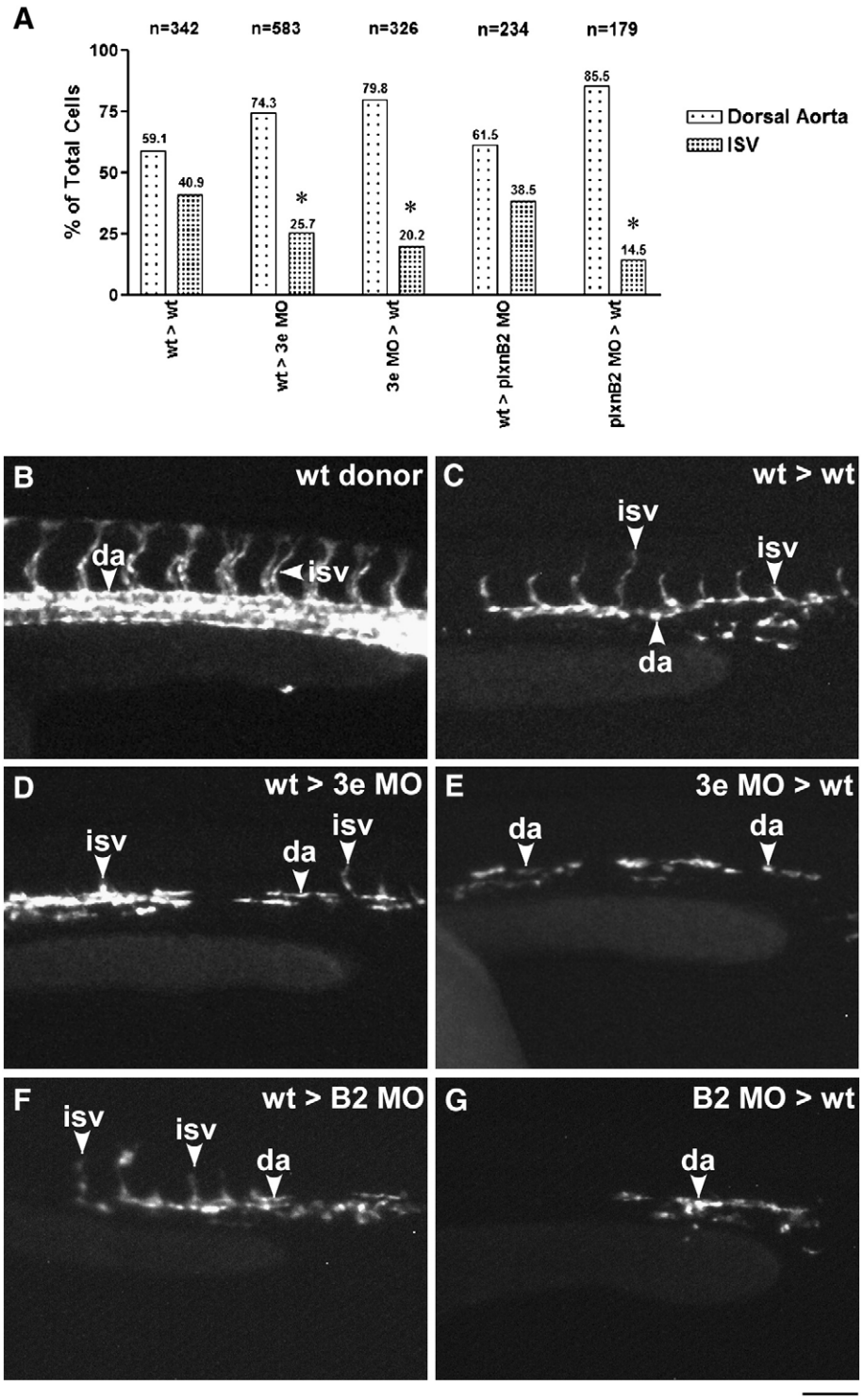

Fig. 5. Sema3e acts both autonomously and non-autonomously in angioblasts while PlxnB2 acts autonomously. (A) Summary of the total proportion of cell types observed after transplantation given as a percentage of total cells counted. (B–E) Representative images of a *Tg(kdr:GFP)la116* wild type donor embryo (B), recipient embryo from a wt>wt transplantation (C), recipient embryo from a wt>3e MO transplantation (D), recipient embryo from a 3e MO>wt transplantation (E), recipient from a wt>plxnB2 MO transplantation (F), and recipient from a plxnB2 MO>wt transplantation (G). Arrows indicate cells classified as dorsal aorta (da), ISV cells (ISV). * denotes a probability of difference from wild type by Chi-square test of <0.002. Scale bar is 100 μm.

secreting Sema3e also affects surrounding cells as well as its self, thus appearing to act both cell autonomously and non-autonomously.

To investigate if Sema3e–PlxnB2 signalling is required both cell autonomously, non-autonomously, or both, we transplanted *plxnB2* morphant endothelial cells into wild type recipients, as well as wild type endothelial cells into *plxnB2* morphant recipients, and determined their contribution to either the dorsal aorta of ISV as above. Transplantation of wild type *Tg(kdr:GFP)*^{la116} angioblasts into *plxnB2*^{i10e11} morphant recipients resulted in a cell distribution similar to that observed in control wild type to wild type experiments with 61.5% of cells contributing to the dorsal aorta and 38.5% of cells contributing to the ISVs ($n = 234$ cells from 19 embryos; not significantly different from wt>wt transplants by Chi-square test; Figs. 5A, F). Conversely, when *plxnB2*^{i10e11} morphant *Tg(kdr:GFP)*^{la116}

angioblasts were transplanted into wild type recipients, we observed 85.5% of angioblasts contributed to the dorsal aorta, while only 14.5% of *plxnB2* morphant angioblasts contributed to ISVs ($n = 179$ cells from 20 embryos; $p < 0.001$ by Chi-square test; Figs 5A, G), similar to results observed for *sema3e* morphants.

Discussion

Sema3e controls the timing of intersegmental vessel sprouting independently of PlxnD1

We have uncovered a new role for Sema3e in zebrafish vascular development and present genetic evidence that Sema3e acts primarily through PlxnB2, and not PlxnD1, to control the timing of angioblast sprouting. Previous in vitro and in vivo work in mouse has shown that Sema3e is repulsive to angioblasts, and is a ligand for the plexin receptor, PlxnD1 (Gu et al., 2005). Thus, we hypothesized that zebrafish *sema3e* morphants would share the same vascular phenotype as *obd* mutants. However, this is not the case as *sema3e* morphants show delayed angioblast sprouting while *obd* mutant embryos show precocious sprouting. This suggests that Sema3e plays a novel additional role in vascular development in the control of angioblast migration, independently of its interaction with PlxnD1. The differences between the Sema3e knockdown/knockout phenotypes in mouse and fish could be attributed to species differences in expression and function. Sema3e has not been reported to be expressed in vessels in mice although it is expressed in the motor domain of the neural tube, in non-neural mesenchyme between the neural tube and dorsal root ganglia at embryonic day (E) 12.5, and in the caudal somite at E11.5 (Gu et al., 2005) (Miyazaki et al., 1999b; Zou et al., 2000). With the exception of motor domain expression, we do not find overlapping expression in the fish. In zebrafish *sema3e* is expressed by the large vessels of the trunk, the ISVs, and in the endoderm beneath the pronephric ducts. We find that the level of vascular expression of *sema3e* is weaker than its motoneuron expression in zebrafish, and perhaps further analysis of Sema3e expression in mice will also find it expressed at low levels in vessels.

PlxnB2 genetically interacts with Sema3e to control timing of angioblast sprouting

Since PlxnD1 did not appear to be the receptor for Sema3e in timing angioblast sprouting, we performed an expression screen of all previously uncharacterized zebrafish plexins. Previously, PlxnB2 expression was identified in human umbilical vein endothelial cells in culture (Toyofuku et al., 2007) and here we show that plxnB2 is expressed ubiquitously. *plxnB2* morphants exhibit a phenotype identical to that of *sema3e* morphants with severely delayed angioblast sprouting, suggesting that PlxnB2 might be the receptor for Sema3e in controlling timing of angioblast sprouting. Further, co-injection of sub-optimal doses of morpholinos for *sema3e* and *plxnB2* results in the same delayed angioblast sprouting phenotype as for full doses of each morpholino-injected alone. These data suggest that PlxnB2 could act as a receptor for Sema3e in sprouting angioblasts.

Antagonism among PlxnB2, PlxnD1 and Sema3e

To understand the relationship between PlxnB2 and PlxnD1 in controlling ISV development, we manipulated *sema3e* levels in *obd*/PlxnD1 genetic mutants. If Sema3e and/or PlxnB2 were acting in the same pathway as PlxnD1, we would expect to see no additional exacerbation of the *obd* phenotype when expression of Sema3e or PlxnB2 is lost in *obd*/PlxnD1 mutants. This is not the case as we observe a delay in angioblast sprouting when expression of Sema3e or PlxnB2 is lost in *obd*/PlxnD1 mutants. This delay is less than the delay of *sema3e* or *plxnB2* morphants in a non-*obd* genetic background, but more than wild type animals or *obd* mutants, and thus is intermediate. Therefore PlxnB2 and PlxnD1 likely use independent and opposing signalling pathways to control the timing of angioblast exit.

Sema3e influences angioblast sprouting in both a cell autonomous and non-autonomous manner

Although previous studies have demonstrated Sema3e expression in cultured endothelial cells (Christensen et al., 2005; Serini et al., 2003), our study is the first to identify *sema3e* expression within blood vessels in vivo, and points to a novel role for Sema3e in vascular development. Semaphorin–plexin signalling typically involves non-autonomous interactions between a ligand expressed in the environment and a plexin receptor expressed on a migratory cell. Indeed, PlxnD1 expressed on angioblasts appears to interact with Sema3ab expressed by somites to pattern the direction of ISV growth in zebrafish (Torres-Vazquez et al., 2004).

However, ours is the first example of a semaphorin playing an autonomous role in timing of angioblast sprouting. Cell autonomous roles for semaphorins are only recently being uncovered. Sema3a is expressed in newly forming vessels where it plays a role in adhesion of endothelial cells to different substrates (Serini et al., 2003), while Sema3c expressed by glomerular endothelial cells plays an autocrine role in cell proliferation, adhesion, tube formation, and $VEGF_{120}$ secretion (Banu et al., 2006). Further, semaphorin expression cell autonomously influences other developmental processes such as salivary gland cleft formation (Chung et al., 2007), lung branching morphogenesis (Ito et al., 2000; Kagoshima and Ito, 2001), and podocyte differentiation and survival (Guan et al., 2006).

Our cell transplantation experiments showed that *sema3e* acts both cell autonomously and non-autonomously in angioblasts, a seeming contradiction. *sema3e* morphant angioblasts transplanted into wild type recipients have delayed sprouting, suggesting that autocrine *sema3e* signalling is required during vessel development. But we also show that *sema3e* acts non-cell autonomously on angioblasts because wild type angioblasts transplanted into *sema3e* morphant recipients also have delayed sprouting. In contrast, wild type cells transplanted into wild type embryos have normal sprout timing. In our transplant experiments the only other sources of Sema3e expression in the zebrafish embryo were eliminated by pre-sorting for embryos containing minimal numbers of cells of endodermal or ectodermal origin. Thus, Sema3e appears to be required by both host and donor angioblasts for proper angioblast sprouting.

Transplantation of *plxnB2* morphant angioblasts into a wild type environment resulted in delayed angioblast sprouting similar to that observed for *sema3e* morphant angioblasts. However, the converse experiment of transplanting wild type angioblasts into a *plxnB2* morphant resulted in angioblasts migrating in a pattern similar to those observed in wild type experiments, suggesting that *plxnB2* acts cell autonomously to control the timing of angioblast sprouting. This is not surprising given that PlxnB2 is a transmembrane receptor anchored to the expressing cell, and would be expected to act only on the cell to which it is tethered. We propose that angioblasts forming the ISVs are in physical contact with other angioblasts in the dorsal aorta prior to sprouting and express the PlxnB2 receptor. Our data suggest that a sufficiently high and additive level of Sema3e expression from the local 'community' of angioblasts within a sprout is required to control the timing of sprouting. If any cell within a sprout lacks Sema3e, the migration of the whole sprout is delayed.

A model for the interactions among semaphorin/plexin signalling in ISV development

VEGF is the primary inductive signal for ISV sprouting and is expressed several hours before the first sprouts appear. Plexin–semaphorin signalling on the other hand, modulates the timing and

path of sprouting (Covassin et al., 2006; Lawson et al., 2003; Nasevicius et al., 2000). We have previously shown that the guidance of ISV growth is regulated by the non-autonomous interaction of endothelially-expressed PlxnD1 and somite-expressed semaphorins, such as Sema3a2. Further, PlexinD1 also represses ISV sprouting since *out of bounds* mutant embryos have precocious sprouting (Childs et al., 2002; Torres-Vazquez et al., 2004). Here we show that the promotion of sprouting is regulated by the interaction of endothelially-expressed Sema3e and endothelially-expressed PlxnB2. Since PlxnD1 and PlxnB2 have apparently antagonistic effects on the timing of sprouting, do both receptor signalling pathways act in parallel to converge on the same downstream signalling molecules or does the activation of one receptor modify the signalling of the other? Plexin family members interact with, and signal through, small GTPases of the Rnd and R-Ras families to modify integrin adhesion (Oinuma et al., 2004; Uesugi et al., 2009). While PlxnB2 interacts with Rnd1, PlxnD1 interacts with Rnd2 (Chardin, 2006). The interactions between Rnd1 or Rnd2 and R-Ras are not completely elucidated, but if they had differing abilities to activate R-Ras, this would provide a possible direct mechanism for how PlxnB2 and PlxnD1 signal antagonistically.

There is also precedent for modulation of sensitivity in semaphorin signalling. Overexpression of Sema3A within chick spinal motoneurons desensitizes their growing axons to environmental Sema3A, allowing inappropriate axon growth into regions normally repulsive to these axons. Further, loss of Sema3A in these axons makes axons highly sensitive to environmentally expressed Sema3A (Moret et al., 2007). The striking delay of angioblast sprouting observed in *sema3e* morphants could result from increased sensitivity of angioblasts lacking Sema3e to repulsive cues expressed in the environment such as Sema3a. Future experiments will allow us to distinguish the precise mechanism by which the two receptors modulate each other's signalling to finely tune the timing of angiogenic sprouting.

Acknowledgments

RL is the recipient of a Heart and Stroke Foundation of Canada Studentship. SJC is an AHFMR Senior Scholar, a Heart and Stroke Foundation of Canada Scholar and a Tier 2 Canada Research Chair. Funding for this work was provided by an operating grant from the Canadian Institutes for Health Research (MOP 53230). We thank Olivera Starovic-Subota for assistance with sectioning and Jau-Nian Chen for *Tg(kdr:GFP)*^{la116} zebrafish and the *kdr* promoter construct. We thank Sarah McFarlane, Erica Watson, and Tara Christie for helpful comments on the manuscript.

Appendix A. Supplementary data

Supplementary data associated with this article can be found in the online version at doi:10.1016/j.ydbio.2009.04.037.

References

Adams, R.H., Lohrum, M., Klostermann, A., Betz, H., Puschel, A.W., 1997. The chemorepulsive activity of secreted semaphorins is regulated by furin-dependent proteolytic processing. EMBO J. 16, 6077–6086.

Artigiani, S., Barberis, D., Fazzari, P., Longati, P., Angelini, P., van de Loo, J.W., Comoglio, P.M., Tamagnone, L., 2003. Functional regulation of semaphorin receptors by proprotein convertases. J. Biol. Chem. 278, 10094–10101.

Aurandt, J., Vikis, H.G., Gutkind, J.S., Ahn, N., Guan, K.L., 2002. The semaphorin receptor plexin-B1 signals through a direct interaction with the Rho-specific nucleotide exchange factor, LARG. Proc. Natl. Acad. Sci. U. S. A. 99, 12085–12090.

Banu, N., Teichman, J., Dunlap-Brown, M., Villegas, G., Tufro, A., 2006. Semaphorin 3C regulates endothelial cell function by increasing integrin activity. FASEB J. 20, 2150–2152.

Basile, J.R., Barac, A., Zhu, T., Guan, K.L., Gutkind, J.S., 2004. Class IV semaphorins promote angiogenesis by stimulating Rho-initiated pathways through plexin-B. Cancer Res. 64, 5212–5224.

Callander, D.C., Lamont, R.E., Childs, S.J., McFarlane, S., 2007. Expression of multiple class three semaphorins in the retina and along the path of zebrafish retinal axons. Dev. Dyn. 236, 2918–2924.

Chardin, P., 2006. Function and regulation of Rnd proteins. Nat. Rev. Mol. Cell. Biol. 7, 54–62.

Chauvet, S., Cohen, S., Yoshida, Y., Fekrane, L., Livet, J., Gayet, O., Segu, L., Buhot, M.C., Jessell, T.M., Henderson, C.E., Mann, F., 2007. Gating of Sema3E/PlexinD1 signaling by neuropilin-1 switches axonal repulsion to attraction during brain development. Neuron 56, 807–822.

Childs, S., Chen, J.N., Garrity, D.M., Fishman, M.C., 2002. Patterning of angiogenesis in the zebrafish embryo. Development 129, 973–982.

Choi, J., Dong, L., Ahn, J., Dao, D., Hammerschmidt, M., Chen, J.N., 2007. FoxH1 negatively modulates flk1 gene expression and vascular formation in zebrafish. Dev. Biol. 304, 735–744.

Christensen, C., Ambartsumian, N., Gilestro, G., Thomsen, B., Comoglio, P., Tamagnone, L., Guldberg, P., Lukanidin, E., 2005. Proteolytic processing converts the repelling signal Sema3E into an inducer of invasive growth and lung metastasis. Cancer Res. 65, 6167–6177.

Chung, L., Yang, T.L., Huang, H.R., Hsu, S.M., Cheng, H.J., Huang, P.H., 2007. Semaphorin signaling facilitates cleft formation in the developing salivary gland. Development 134, 2935–2945.

Covassin, L.D., Villefranc, J.A., Kacergis, M.C., Weinstein, B.M., Lawson, N.D., 2006. Distinct genetic interactions between multiple Vegf receptors are required for development of different blood vessel types in zebrafish. Proc. Natl. Acad. Sci. U. S. A. 103, 6554–6559.

Cross, L.M., Cook, M.A., Lin, S., Chen, J.N., Rubinstein, A.L., 2003. Rapid analysis of angiogenesis drugs in a live fluorescent zebrafish assay. Arterioscler. Thromb. Vasc. Biol. 23, 911–912.

Deng, S., Hirschberg, A., Worzfeld, T., Penachioni, J.Y., Korostylev, A., Swiercz, J.M., Vodrazka, P., Mauti, O., Stoeckli, E.T., Tamagnone, L., Offermanns, S., Kuner, R., 2007. Plexin-B2, but not Plexin-B1, critically modulates neuronal migration and patterning of the developing nervous system in vivo. J. Neurosci. 27, 6333–6347.

Du, S.J., Gao, J., Anyangwe, V., 2003. Muscle-specific expression of myogenin in zebrafish embryos is controlled by multiple regulatory elements in the promoter. Comp. Biochem. Physiol., B. Biochem. Mol. Biol. 134, 123–134.

Eichmann, A., Makinen, T., Alitalo, K., 2005. Neural guidance molecules regulate vascular remodeling and vessel navigation. Genes Dev. 19, 1013–1021.

Eriksson, J., Lofberg, J., 2000. Development of the hypochord and dorsal aorta in the zebrafish embryo (*Danio rerio*). J. Morphol. 244, 167–176.

Friedel, R.H., Kerjan, G., Rayburn, H., Schuller, U., Sotelo, C., Tessier-Lavigne, M., Chedotal, A., 2007. Plexin-B2 controls the development of cerebellar granule cells. J. Neurosci. 27, 3921–3932.

Gerhardt, H., Golding, M., Fruttiger, M., Ruhrberg, C., Lundkvist, A., Abramsson, A., Jeltsch, M., Mitchell, C., Alitalo, K., Shima, D., Betsholtz, C., 2003. VEGF guides angiogenic sprouting utilizing endothelial tip cell filopodia. J. Cell Biol. 161, 1163–1177.

Gitler, A.D., Lu, M.M., Epstein, J.A., 2004. PlexinD1 and semaphorin signaling are required in endothelial cells for cardiovascular development. Dev. Cell 7, 107–116.

Gu, C., Yoshida, Y., Livet, J., Reimert, D.V., Mann, F., Merte, J., Henderson, C.E., Jessell, T.M., Kolodkin, A.L., Ginty, D.D., 2005. Semaphorin 3E and plexin-D1 control vascular pattern independently of neuropilins. Science 307, 265–268.

Guan, F., Villegas, G., Teichman, J., Mundel, P., Tufro, A., 2006. Autocrine class 3 semaphorin system regulates slit diaphragm proteins and podocyte survival. Kidney Int. 69, 1564–1569.

Hartwig, C., Veske, A., Krejcova, S., Rosenberger, G., Finckh, U., 2005. Plexin B3 promotes neurite outgrowth, interacts homophilically, and interacts with Rin. BMC Neurosci. 6, 53.

Hellstrom, M., Phng, L.K., Hofmann, J.J., Wallgard, E., Coultas, L., Lindblom, P., Alva, J., Nilsson, A.K., Karlsson, L., Gaiano, N., Yoon, K., Rossant, J., Iruela-Arispe, M.L., Kalen, M., Gerhardt, H., Betsholtz, C., 2007. Dll4 signalling through Notch1 regulates formation of tip cells during angiogenesis. Nature 445, 776–780.

Herzog, Y., Guttmann-Raviv, N., Neufeld, G., 2005. Segregation of arterial and venous markers in subpopulations of blood islands before vessel formation. Dev. Dyn. 232, 1047–1055.

Ito, T., Kagoshima, M., Sasaki, Y., Li, C., Udaka, N., Kitsukawa, T., Fujisawa, H., Taniguchi, M., Yagi, T., Kitamura, H., Goshima, Y., 2000. Repulsive axon guidance molecule Sema3A inhibits branching morphogenesis of fetal mouse lung. Mech. Dev. 97, 35–45.

Jowett, T., Lettice, L., 1994. Whole-mount in situ hybridizations on zebrafish embryos using a mixture of digoxigenin- and fluorescein-labelled probes. Trends Genet. 10, 73–74.

Kagoshima, M., Ito, T., 2001. Diverse gene expression and function of semaphorins in developing lung: positive and negative regulatory roles of semaphorins in lung branching morphogenesis. Genes Cells 6, 559–571.

Kimmel, C.B., Ballard, W.W., Kimmel, S.R., Ullmann, B., Schilling, T.F., 1995. Stages of embryonic development of the zebrafish. Dev. Dyn. 203, 253–310.

Kwan, K.M., Fujimoto, E., Grabher, C., Mangum, B.D., Hardy, M.E., Campbell, D.S., Parant, J.M., Yost, H.J., Kanki, J.P., Chien, C.B., 2007. The Tol2kit: a multisite gateway-based construction kit for Tol2 transposon transgenesis constructs. Dev. Dyn. 236, 3088–3099.

Lawson, N.D., Weinstein, B.M., 2002. In vivo imaging of embryonic vascular development using transgenic zebrafish. Dev. Biol. 248, 307–318.

Lawson, N.D., Mugford, J.W., Diamond, B.A., Weinstein, B.M., 2003. Phospholipase C gamma-1 is required downstream of vascular endothelial growth factor during arterial development. Genes Dev. 17, 1346–1351.

Leslie, J.D., Ariza-McNaughton, L., Bermange, A.L., McAdow, R., Johnson, S.L., Lewis, J., 2007. Endothelial signalling by the Notch ligand delta-like 4 restricts angiogenesis. Development 134, 839–844.

Miyazaki, N., Furuyama, T., Amasaki, M., Sugimoto, H., Sakai, T., Takeda, N., Kubo, T., Inagaki, S., 1999a. Mouse semaphorin H inhibits neurite outgrowth from sensory neurons. Neurosci. Res. 33, 269–274.

Miyazaki, N., Furuyama, T., Sakai, T., Fujioka, S., Mori, T., Ohoka, Y., Takeda, N., Kubo, T., Inagaki, S., 1999b. Developmental localization of semaphorin H messenger RNA acting as a collapsing factor on sensory axons in the mouse brain. Neuroscience 93, 401–408.

Moret, F., Renaudot, C., Bozon, M., Castellani, V., 2007. Semaphorin and neuropilin co-expression in motoneurons sets axon sensitivity to environmental semaphorin sources during motor axon pathfinding. Development 134, 4491–4501.

Nasevicius, A., Larson, J., Ekker, S.C., 2000. Distinct requirements for zebrafish angiogenesis revealed by a VEGF-A morphant. Yeast 17, 294–301.

Oinuma, I., Ishikawa, Y., Katoh, H., Negishi, M., 2004. The Semaphorin 4D receptor Plexin-B1 is a GTPase activating protein for R-Ras. Science 305, 862–865.

Perrot, V., Vazquez-Prado, J., Gutkind, J.S., 2002. Plexin B regulates Rho through the guanine nucleotide exchange factors leukemia-associated Rho GEF (LARG) and PDZ-RhoGEF. J. Biol. Chem. 277, 43115–43120.

Pozas, E., Pascual, M., Nguyen Ba-Charvet, K.T., Guijarro, P., Sotelo, C., Chedotal, A., Del Rio, J.A., Soriano, E., 2001. Age-dependent effects of secreted semaphorins 3A, 3F, and 3E on developing hippocampal axons: in vitro effects and phenotype of Semaphorin 3A (−/−) mice. Mol. Cell. Neurosci. 18, 26–43.

Robu, M.E., Larson, J.D., Nasevicius, A., Beiraghi, S., Brenner, C., Farber, S.A., Ekker, S.C., 2007. p53 Activation by knockdown technologies. PLoS Genet. 3, e78.

Serini, G., Valdembri, D., Zanivan, S., Morterra, G., Burkhardt, C., Caccavari, F., Zammataro, L., Primo, L., Tamagnone, L., Logan, M., Tessier-Lavigne, M., Taniguchi, M., Puschel, A.W., Bussolino, F., 2003. Class 3 semaphorins control vascular morphogenesis by inhibiting integrin function. Nature 424, 391–397.

Siekmann, A.F., Lawson, N.D., 2007. Notch signalling limits angiogenic cell behaviour in developing zebrafish arteries. Nature 445, 781–784.

Steffensky, M., Steinbach, K., Schwarz, U., Schlosshauer, B., 2006. Differential impact of semaphorin 3E and 3A on CNS axons. Int. J. Dev. Neurosci. 24, 65–72.

Steinbach, K., Volkmer, H., Schlosshauer, B., 2002. Semaphorin 3E/collapsin-5 inhibits growing retinal axons. Exp. Cell. Res. 279, 52–61.

Swiercz, J.M., Kuner, R., Behrens, J., Offermanns, S., 2002. Plexin-B1 directly interacts with PDZ-RhoGEF/LARG to regulate RhoA and growth cone morphology. Neuron 35, 51–63.

Takahashi, T., Fournier, A., Nakamura, F., Wang, L.H., Murakami, Y., Kalb, R.G., Fujisawa, H., Strittmatter, S.M., 1999. Plexin-neuropilin-1 complexes form functional semaphorin-3A receptors. Cell 99, 59–69.

Tamagnone, L., Artigiani, S., Chen, H., He, Z., Ming, G.I., Song, H., Chedotal, A., Winberg, M.L., Goodman, C.S., Poo, M., Tessier-Lavigne, M., Comoglio, P.M., 1999. Plexins are a large family of receptors for transmembrane, secreted, and GPI-anchored semaphorins in vertebrates. Cell 99, 71–80.

Torres-Vazquez, J., Gitler, A.D., Fraser, S.D., Berk, J.D., Van, N.P., Fishman, M.C., Childs, S., Epstein, J.A., Weinstein, B.M., 2004. Semaphorin–plexin signaling guides patterning of the developing vasculature. Dev. Cell. 7, 117–123.

Toyofuku, T., Yabuki, M., Kamei, J., Kamei, M., Makino, N., Kumanogoh, A., Hori, M., 2007. Semaphorin-4A, an activator for T-cell-mediated immunity, suppresses angiogenesis via Plexin-D1. EMBO J. 26, 1373–1384.

Uesugi, K., Oinuma, I., Katoh, H., Negishi, M., 2009. Different requirement for Rnd GTPases of R-Ras GAP activity of Plexin-C1 and Plexin-D1. J. Biol. Chem. 284, 6743–6751.

Westerfield, M., 1995. The Zebrafish Book: A Guide for the Laboratory use of Zebrafish (Danio rerio).

Winberg, M.L., Noordermeer, J.N., Tamagnone, L., Comoglio, P.M., Spriggs, M.K., Tessier-Lavigne, M., Goodman, C.S., 1998. Plexin A is a neuronal semaphorin receptor that controls axon guidance. Cell 95, 903–916.

Zhu, H., Traver, D., Davidson, A.J., Dibiase, A., Thisse, C., Thisse, B., Nimer, S., Zon, L.I., 2005. Regulation of the lmo2 promoter during hematopoietic and vascular development in zebrafish. Dev. Biol. 281, 256–269.

Zou, Y., Stoeckli, E., Chen, H., Tessier-Lavigne, M., 2000. Squeezing axons out of the gray matter: a role for slit and semaphorin proteins from midline and ventral spinal cord. Cell 102, 363–375.